Magnetic Reconnection with Asymmetry in the Outflow Direction

Nicholas Murphy,[1] Carl Sovinec,[2] and Paul Cassak[3]

[1]Department of Astronomy, University of Wisconsin, Madison, WI

[2]Department of Engineering Physics, University of Wisconsin, Madison, WI

[3]Department of Physics, West Virginia University, Morgantown, WV

50th Annual Meeting of the APS Division of Plasma Physics

November 17-21, 2008

Dallas, Texas

Outline

- Motivation for studying reconnection with asymmetry in the outflow direction
- Presentation of the equations of steady-state resistive MHD in surface integral form
- Review of Sweet-Parker reconnection when pressure effects and compressibility are included
- Control volume analysis of reconnection with asymmetric downstream pressure
- Control volume analysis of reconnection in toroidal geometry with the outflow aligned with the radial direction
- Numerical tests of this model in straight and toroidal geometries

Reconnection with asymmetry in the outflow direction

- Reconnection in physically realistic scenarios will often have asymmetry in the outflow direction
  - Current sheets in the near-Earth magnetotail
  - Coronal mass ejections and some solar flares
  - Laboratory merging of toroidal plasma configurations (e.g., SSX, MRX, TS-3/4/5)
  - Magnetically channeled disks in the winds of massive stars
  - Reconnection during turbulence or reconnection with multiple competing islands
- Cassak & Shay (2007) extend the Sweet-Parker model to describe reconnection between plasmas with different upstream magnetic field strengths and/or different densities
- We perform a similar analysis for reconnection with asymmetric downstream pressure

Resistive MHD model

- The equations of resistive MHD in conservative form are

$$\frac{\partial \rho}{\partial t} + \nabla \cdot (\rho \mathbf{V}) = 0 \tag{1}$$

$$\frac{\partial (\rho \mathbf{V})}{\partial t} + \nabla \cdot \left[\rho \mathbf{V}\mathbf{V} + \left(p + \frac{B^2}{2\mu_0} \right) \hat{\mathbf{I}} - \frac{\mathbf{B}\mathbf{B}}{\mu_0} \right] = 0 \tag{2}$$

$$\frac{\partial e}{\partial t} + \nabla \cdot \left[\left(\frac{\rho V^2}{2} + \frac{\gamma}{\gamma - 1} p \right) \mathbf{V} + \frac{\mathbf{E} \times \mathbf{B}}{\mu_0} \right] = 0 \tag{3}$$

$$\frac{\partial \mathbf{B}}{\partial t} + \nabla \times \mathbf{E} = 0 \tag{4}$$

$$\mu_0 \mathbf{J} = \nabla \times \mathbf{B} \tag{5}$$

$$\mathbf{E} + \mathbf{V} \times \mathbf{B} = \eta \mathbf{J} \tag{6}$$

- In order, these represent conservation of mass, momentum, and energy, Faraday's law, Ampere's law without displacement current, and Ohm's law, with $e \equiv \rho V^2/2 + p/(\gamma - 1) + B^2/2\mu_0$

Equations of steady-state MHD in integral form

- With the help of Gauss' and Stokes' theorems, the equations of steady-state resistive MHD can be written as

$$\oint_S d\mathbf{S} \cdot (\rho \mathbf{V}) = 0 \tag{7}$$

$$\oint_S d\mathbf{S} \cdot \left[\rho \mathbf{V}\mathbf{V} + \left(p + \frac{B^2}{2\mu_0}\right)\hat{\mathbf{I}} - \frac{\mathbf{B}\mathbf{B}}{\mu_0}\right] = 0 \tag{8}$$

$$\oint_S d\mathbf{S} \cdot \left[\left(\frac{\rho V^2}{2} + \frac{\gamma p}{\gamma - 1}\right)\mathbf{V} + \left(\frac{\mathbf{E} \times \mathbf{B}}{\mu_0}\right)\right] = 0 \tag{9}$$

$$\oint_S d\mathbf{S} \times \mathbf{E} = 0 \tag{10}$$

- In order, these represent conservation of mass, momentum, energy, and flux (e.g., Goedbloed & Poedts 2004)
- These relations are valid for any closed volume in steady-state MHD

Symmetric downstream pressure

- The effects of symmetric downstream pressure have been analyzed in Chapter 4 of Priest & Forbes (2000). We repeat this analysis without assuming incompressibility.
- Conservation of mass gives

$$\rho_{in} V_{in} L \sim \rho_{out} V_{out} \delta \tag{11}$$

- Defining $\alpha \equiv \gamma/(\gamma-1)$ and using $E_y = V_{in} B_{in}$, conservation of energy gives

$$V_{in} L \left(\alpha p_{in} + \frac{B_{in}^2}{\mu_0} \right) \sim V_{out} \delta \left(\frac{\rho_{out} V_{out}^2}{2} + \alpha p_{out} \right) \tag{12}$$

- Defining $V_A \equiv B_{in}/\sqrt{\mu_0 \rho_{in}}$, the outflow velocity is then given by

$$V_{out}^2 \sim 2 V_A^2 - 2\alpha \left(\frac{p_{out}}{\rho_{out}} - \frac{p_{in}}{\rho_{in}} \right) \tag{13}$$

Symmetric downstream pressure (cont.)

- The outflow will be given by $V_{out} \sim V_A$ when

(14) $$\alpha \left[p_{out} \left(\frac{\rho_{in}}{\rho_{out}} \right) - p_{in} \right] \sim \frac{B_{in}^2}{2\mu_0}$$

- The results so far are independent of dissipation mechanism, but to derive a reconnection rate, we now assume resistive dissipation
- Because $E_y = V_{in} B_{in}$ is constant and $J_y \sim B_{in}/\delta$, the inflow velocity is given by

(15) $$V_{in} \sim \frac{\eta}{\mu_0 \delta}$$

- Using conservation of mass and that $S \equiv \mu_0 L V_A / \eta$, we see that

(16) $$\frac{V_{in}}{V_A} \sim \frac{\rho_{out}}{\rho_{in}} \frac{\delta}{L} \frac{V_{out}}{V_A} \Longrightarrow \frac{V_{in}}{V_A} \sim \sqrt{\frac{\rho_{out}}{\rho_{in}} \frac{V_{out}}{V_A} \frac{1}{S}}$$

Symmetric downstream pressure (cont.)

- The reconnection rate for compressible Sweet-Parker-like reconnection is then given by

$$\frac{V_{in}}{V_A} \sim \frac{2^{1/4}}{S^{1/2}} \sqrt{\frac{\rho_{out}}{\rho_{in}}} \left[1 - \frac{\alpha}{2} \left(\frac{p_{out} \left(\rho_{in}/\rho_{out} \right) - p_{in}}{B_{in}^2/2\mu_0} \right) \right]^{1/4} \tag{17}$$

- In this analysis, we include the full Poynting flux rather than just the inflowing magnetic energy
- Reconnection will not be able to occur when

$$\frac{B_{in}^2}{2\mu_0} \lesssim \frac{\alpha}{2} \left[p_{out} \left(\frac{\rho_{in}}{\rho_{out}} \right) - p_{in} \right] \tag{18}$$

- Compressibility effects can reduce the bottleneck caused by conservation of mass
- The reconnection rate is weakly sensitive to downstream pressure because the current sheet width δ is allowed to increase

Modifying the S-P analysis for asymmetric outflow

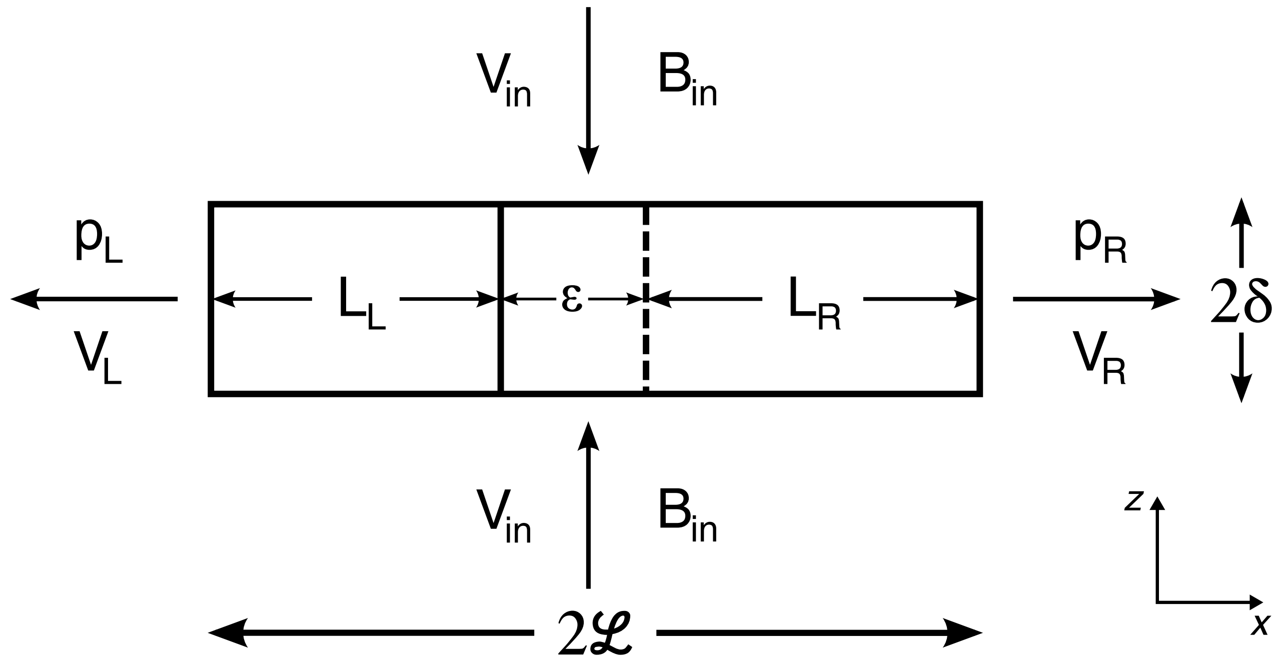

- The above figure represents a current sheet with asymmetric downstream pressure ($p_L > p_R$).
- The current sheet length is given by $2\mathcal{L} \equiv L_L + \epsilon + L_R$.
- The solid vertical bar represents the flow stagnation point, and the dashed bar represents the magnetic field null.
- We assume the reconnection process is externally driven in such a way that the current sheet position remains static.

Finding scaling relations for asymmetric outflow

- We evaluate the surface integrals given in Eqs. 7–10 over the entire current sheet
- Conservation of mass gives

$$2\rho_{in}V_{in}\mathcal{L} \sim \rho_L V_L \delta + \rho_R V_R \delta \tag{19}$$

- Conservation of momentum in the outflow direction gives

$$\rho_L V_L^2 + p_L \sim \rho_R V_R^2 + p_R \tag{20}$$

- Ignoring upstream kinetic energy and downstream magnetic energy, conservation of energy gives

$$2V_{in}\mathcal{L}\left(\alpha p_{in} + \frac{B_{in}^2}{\mu_0}\right) \sim V_L\delta\left(\alpha p_L + \frac{\rho_L V_L^2}{2}\right) + V_R\delta\left(\alpha p_R + \frac{\rho_R V_R^2}{2}\right) \tag{21}$$

Finding a cubic relationship for V_L^2 as a function of p_L and p_R

- By using conservation of mass to eliminate $2\mathcal{L}V_{in}$ and conservation of momentum to eliminate V_R in the relationship for conservation of energy, we arrive at the cubic relationship in V_L^2

$$0 \sim C_{6L}V_L^6 + C_{4L}V_L^4 + C_{2L}V_L^2 + C_{0L} \tag{22}$$

  The expressions for the coefficients are given on the next slide.
- This can be solved analytically using Cardano's method, or numerically by root-solving
- The above relation depends on downstream parameters including density and pressure
- The above expression does not depend on dissipation mechanism, but it does assume a single-fluid framework

Coefficients for the cubic relationship for V_L^2

$$
\begin{aligned}
C_{0L} &\equiv \frac{\rho_R}{\rho_{in}^2}\left(\alpha p_{in} + \frac{B_{in}^2}{\mu_0}\right)^2 (p_L - p_R) \\
&\quad + \left(\alpha p_{in} + \frac{B_{in}^2}{\mu_0}\right)\left(\frac{p_R - p_L}{\rho_{in}}\right)(p_L + 2\alpha p_R - p_R) \\
&\quad + \left(\frac{p_L - p_R}{4\rho_R}\right)(p_L + 2\alpha p_R - p_R)^2
\end{aligned} \tag{23}
$$

$$
\begin{aligned}
C_{2L} &\equiv \left(\alpha p_{in} + \frac{B_{in}^2}{\mu_0}\right)^2 \frac{\rho_L(\rho_R - \rho_L)}{\rho_{in}^2} \\
&\quad + \left(\alpha p_{in} + \frac{B_{in}^2}{\mu_0}\right)\frac{2\rho_L(p_R - p_L)(1-\alpha)}{\rho_{in}} \\
&\quad + \frac{\rho_L}{4\rho_R}(p_L + 2\alpha p_R - p_R)(3p_L - 3p_R + 2\alpha p_R) - \alpha^2 p_L^2
\end{aligned} \tag{24}
$$

$$
C_{4L} \equiv \frac{\rho_L^2}{\rho_R}\left[\frac{3}{4}(p_L - p_R) + \alpha p_R\right] - \alpha p_L \rho_L \tag{25}
$$

$$
C_{6L} \equiv \frac{1}{4}\left(\frac{\rho_L^3}{\rho_R} - \rho_L^2\right) \tag{26}
$$

A simpler result is found by assuming incompressibility

- By assuming incompressibility ($\rho_L = \rho_R = \rho_{in} \equiv \rho$, $\alpha \to 1$), the cubic polynomial in V_L^2 reduces to

(27) $$0 \sim V_L^4 + C_2 V_L^2 + C_0.$$

Here, the coefficient C_{2L} is given by

(28) $$C_{2L} \equiv \frac{p_L - p_R}{\rho},$$

and the coefficient C_{0L} is given by

(29) $$C_{0L} \equiv 4p_{in}\left(\frac{p_L + p_R}{\rho^2}\right) - \left(\frac{2p_{in}}{\rho}\right)^2 - \left(\frac{p_L + p_R}{\rho}\right)^2 + 4V_A^2\left(\frac{p_L + p_R - 2p_{in}}{\rho}\right) - 4V_A^4.$$

- This result is less accurate, but more illustrative and with fewer free parameters

Deriving the outflow velocities (incompressible case)

- An expression for V_L^2 is easily found,

$$V_L^2 \sim -\frac{C_{2L}}{2} + \frac{\sqrt{C_{2L}^2 - 4C_{0L}}}{2}. \tag{30}$$

- Then, using conservation of momentum, V_R^2 is given by

$$V_R^2 \sim V_L^2 + \left(\frac{p_L - p_R}{\rho}\right). \tag{31}$$

- By assuming resistive dissipation, the reconnection rate can be expressed as

$$\frac{V_{in}}{V_A} = \sqrt{\frac{V_L + V_R}{2V_A S}} \tag{32}$$

after V_L and V_R have been found.

Solution plots for $|V_L|$ and $S^{1/2}V_{in}/V_A$ (incompressible case)

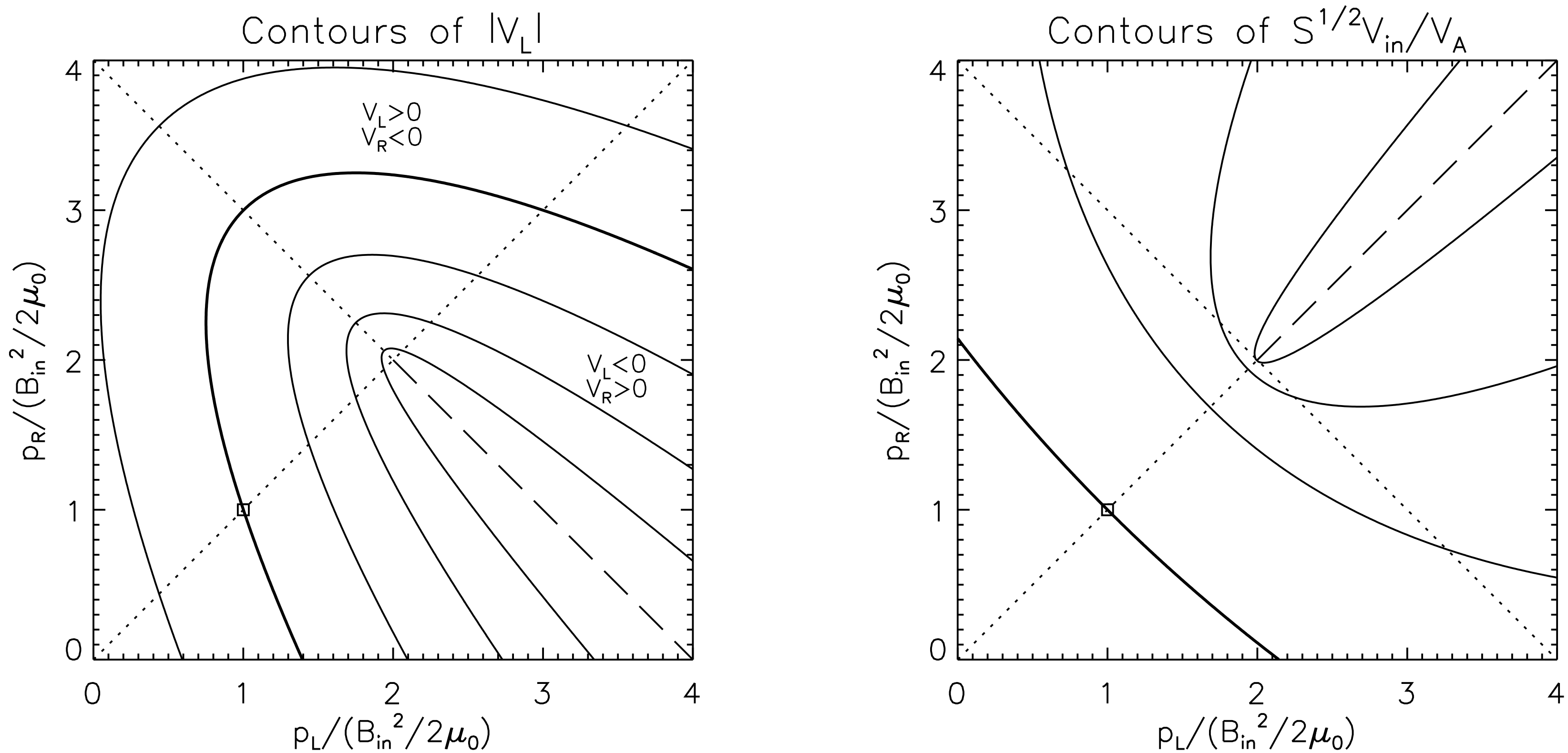

- *Left:* Solution contours for the magnitude of the leftward-directed outflow velocity $|V_L|$ as a function of p_L and p_R with $p_{in} = 0$. Contours are separated by 0.25V_A. The dashed line represents when $V_L = 0$.
- *Right:* Solution contours for the normalized reconnection rate $S^{1/2}V_{in}/V_A$. Contours are separated by 0.25. The dashed line represents when $S^{1/2}V_{in}/V_A = 0$.
- The reconnection rate is greatly affected only when outflow from both sides of the current sheet is blocked. The current sheet width δ is longer for greater downstream pressure.

The flow stagnation point is found through conservation of mass

- Conservation of mass inside the current sheet gives the relations

$$\rho_{in} V_{in} L_L \sim \rho_L V_L \delta, \tag{33}$$

$$\rho_{in} V_{in} \left(\epsilon + L_R\right) \sim \rho_R V_R \delta, \tag{34}$$

where V_n is the flow velocity at the magnetic field null.

- The position of the flow stagnation point is then given by

$$L_L \sim 2\mathcal{L} \left(\frac{\rho_L V_L}{\rho_L V_L + \rho_R V_R} \right), \tag{35}$$

$$\epsilon + L_R \sim 2\mathcal{L} \left(\frac{\rho_R V_R}{\rho_L V_L + \rho_R V_R} \right). \tag{36}$$

The magnetic field null is approximated with the momentum equation

- The outflow component of the momentum equation (ignoring magnetic pressure) is given by

(37) $$\rho V_x \frac{\partial V_x}{\partial x} = \frac{B_z}{\mu_0} \frac{\partial B_x}{\partial z} - \frac{\partial p}{\partial x}$$

- Evaluating this at the flow stagnation point, x_s, and using $\partial B_x / \partial z \sim B_{in}/\delta$, we find

(38) $$\frac{B_z(x_s)}{\mu_0} \frac{B_{in}}{\delta} \sim \left. \frac{\partial p}{\partial x} \right|_{x=x_s}$$

- Given that $B_z(x_n) = 0$ at the magnetic field null position, x_n, a Taylor expansion around $x = x_n$ gives $B_z(x_s) = (x_n - x_s) \left. \frac{\partial B_z}{\partial x} \right|_{x_n} + \mathcal{O}[(x_n - x_s)^2]$
- We then approximate the position of the magnetic field null by

(39) $$\epsilon \equiv x_n - x_s \sim -\frac{\mu_0 \delta}{B_{in}} \left(\frac{\partial p / \partial x}{\partial B_z / \partial x} \right)_{x=x_s}$$

- The field null and stagnation point will not coincide unless the pressure gradient is zero at the flow stagnation point in a steady-state
- When the two points are separated, there will be a Poynting flux across the flow stagnation point even though $V = 0$ there.

Toroidal geometry: setup

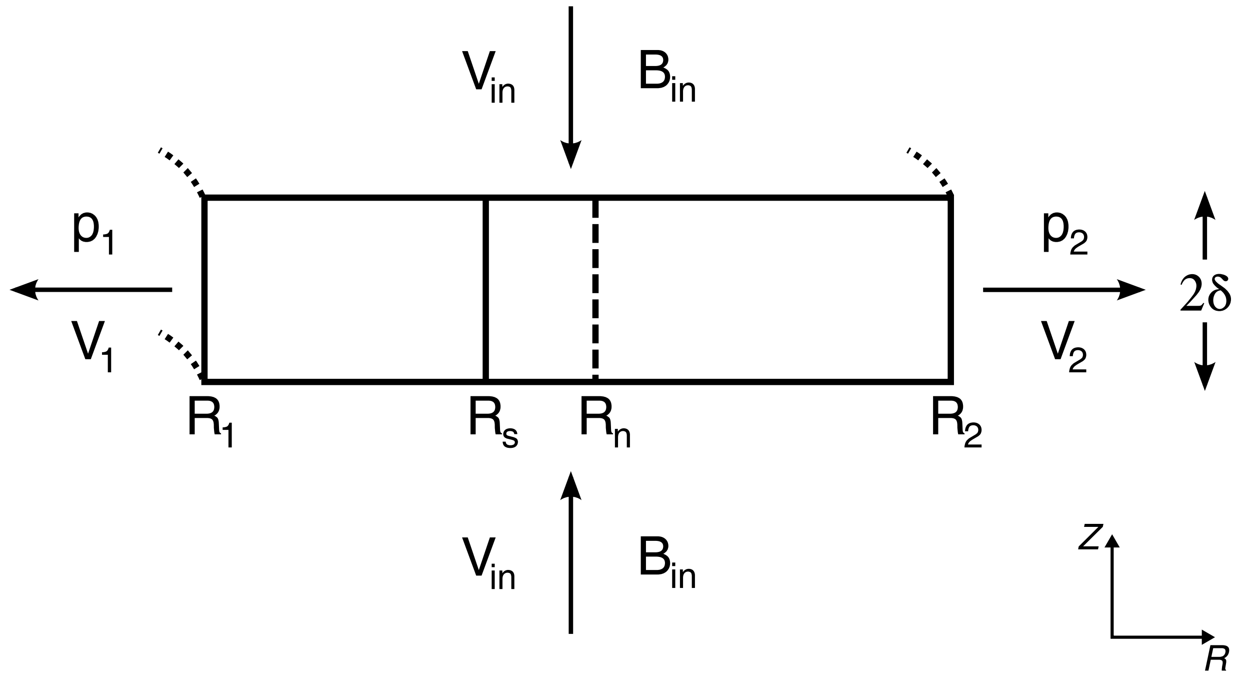

- We also consider reconnection in a toroidal geometry where the outflow is aligned with the radial direction
  - Inflow occurs on two annuli defined by $R \in [R_1, R_2]$ for $Z = \pm\delta$
  - Outflow occurs on two cylinders defined by $Z \in [-\delta, \delta]$ for $R \in \{R_1, R_2\}$
- From the divergence constraint, we assume that the upstream magnetic field takes the form $B_{in}(R) = B_0 R_0 / R$, where B_0 is the magnetic field strength at radius R_0

Toroidal geometry: scaling relations

- By integrating over the entire volume, conservation of mass gives

(40) $$\rho_{in} V_{in} \left(\pi R_2^2 - \pi R_1^2\right) \sim 2\pi R_1 \delta \rho_1 V_1 + 2\pi R_2 \delta \rho_2 V_2$$

- Conservation of momentum gives

(41) $$R_1 \left(\rho_1 V_1^2 + p_1\right) \sim R_2 \left(\rho_2 V_2^2 + p_2\right)$$

- Using $B_{in}(R) = B_0 R_0 / R$, conservation of energy gives

(42) $$\left(\pi R_2^2 - \pi R_1^2\right) V_{in} \alpha p_{in} + \frac{2\pi V_{in} B_0^2 R_0^2}{\mu_0} \ln\left(\frac{R_2}{R_1}\right) \sim$$
$$2\pi R_1 \delta V_1 \left(\frac{\rho_1 V_1^2}{2} + \alpha p_1\right) + 2\pi R_2 \delta V_2 \left(\frac{\rho_2 V_2^2}{2} + \alpha p_2\right)$$

- The inflow velocity and current sheet width remain related by $V_{in} \sim \eta / \mu_0 \delta$

Toroidal geometry: scaling relations (cont.)

- Effects associated with toroidal geometry are applicable to low aspect ratio spheromak merging (SSX, MRX, TS-3/4/5, etc.)
- The relation for momentum balance shows that it is possible to have quicker inward-directed outflow than outward-directed outflow even if the inboard pressure exceeds the outboard pressure
  - This effect has been seen in simulations of MRX (Murphy & Sovinec 2008)
- In these situations, it is not always reasonable to assume that the outflow from both sides of the current sheet will be the same
- Conservation of mass inside the current sheet gives the flow stagnation radius

$$R_s \sim \sqrt{\frac{\rho_1 V_1 R_1 R_2^2 - \rho_2 V_2 R_2 R_1^2}{\rho_1 V_1 R_1 + \rho_2 V_2 R_2}} \tag{43}$$

Testing the model through simulations

- In order to test these models, we perform resistive MHD simulations using the NIMROD finite element code (Sovinec *et al.* 2004)
- The first strategy is to initialize a singly periodic Harris sheet equilibrium with two perturbations closer to each other in one direction than the other
  - The current sheet position is free to move after the current sheets start interacting
- The second strategy is to perform linear geometry simulations using the grid established previously of MRX (Murphy & Sovinec 2008), except with one downstream wall closer than the other downstream wall
  - The driving mechanism constrains the current sheet position
- To test toroidal geometry simulations, we compare the theory developed in this poster with the simulations of MRX in toroidal geometry

Double perturbation simulations of a Harris sheet show X-line retreat

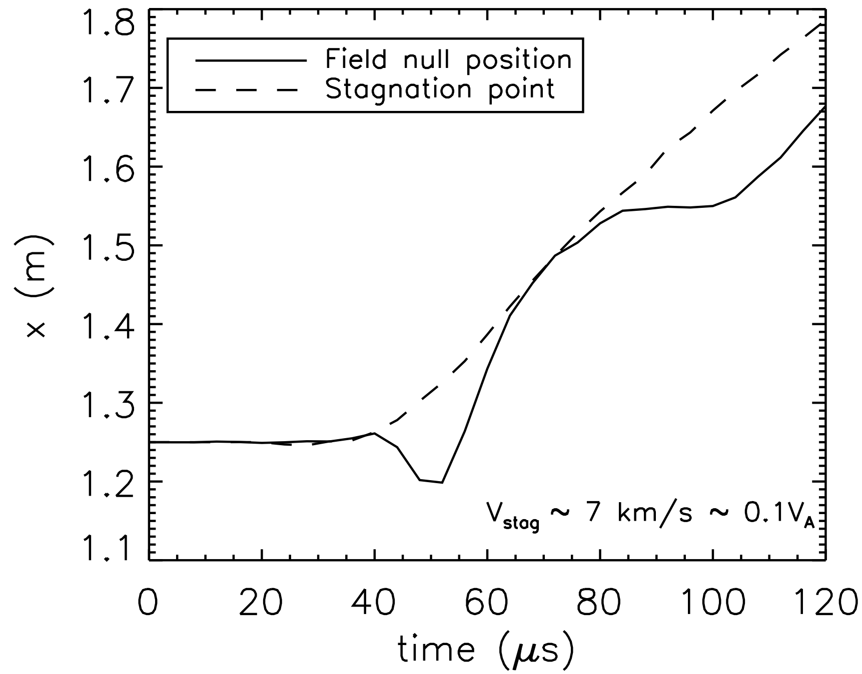

- The position of the current sheet drifts away from the central pressure buildup at $\sim 0.1 V_A$, consistent with kinetic simulations performed by Oka *et al.* in a forthcoming PRL
- Simulation parameters are $B_0 = 250$ G, $V_A \approx 77$ km/s, $\delta_0 = 1$ cm, $B_x = B_0 \tanh(z/\delta_0)$, $S \sim 1000$, $m_i = m_p$, $L \sim 1$ m, $\beta_{in} = 2$, and $n = 5 \times 10^{19}$ m^{-3}

Double perturbation simulations

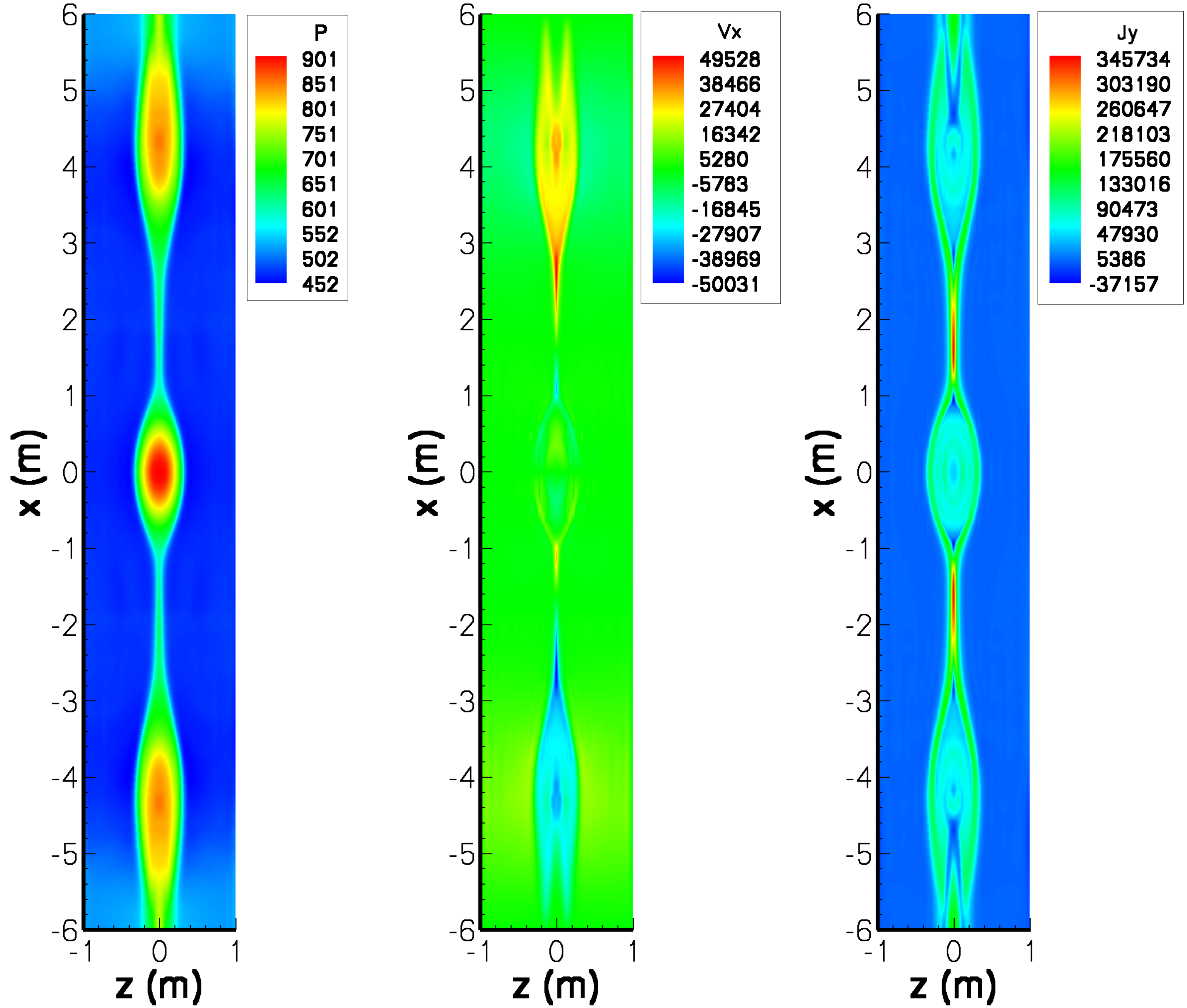

- From left to right are pressure, outflow velocity, and out of plane current density for a singly periodic Harris sheet simulation with two initial perturbations close to each other

Comparison of double perturbation simulation to Eqs. 19–21

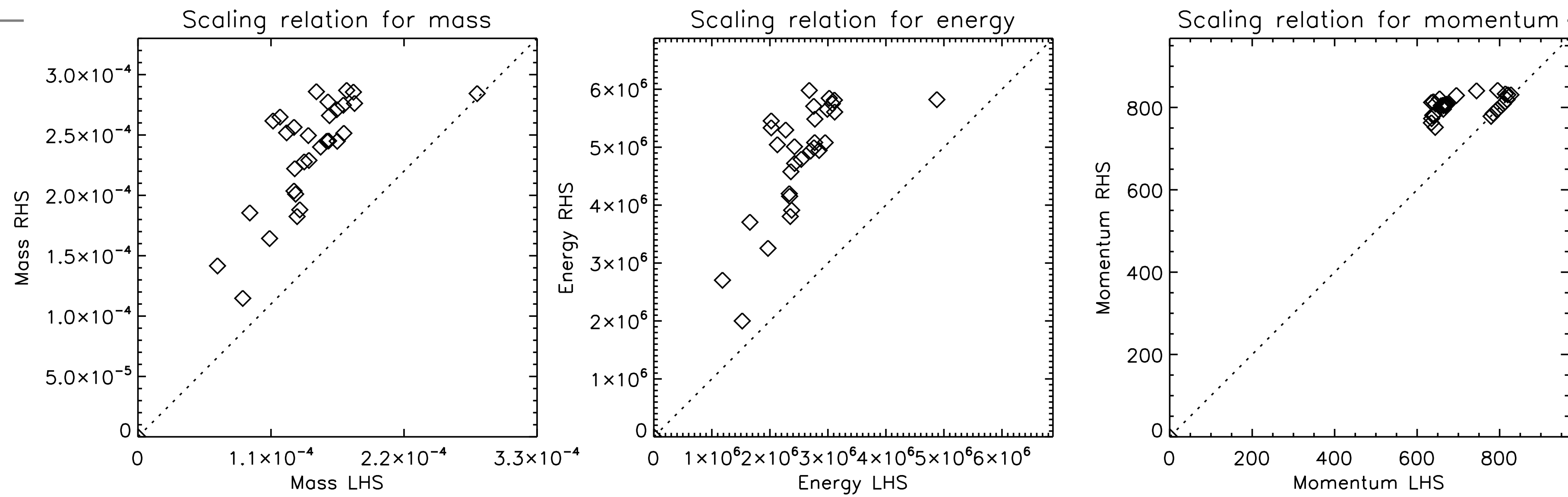

- Conservation of momentum shows good agreement
- Conservation of mass and energy show mediocre agreement, likely due to time-dependent behavior such as X-line retreat and lengthening of the current sheet
- Values were chosen from the simulation at where the current density goes down by a factor of e from its peak value. These points represent different times during the same simulation.
- A voltage application to drive reconnection should help constrain the current sheet's position

We examine simulations of MRX in multiple geometries as a test

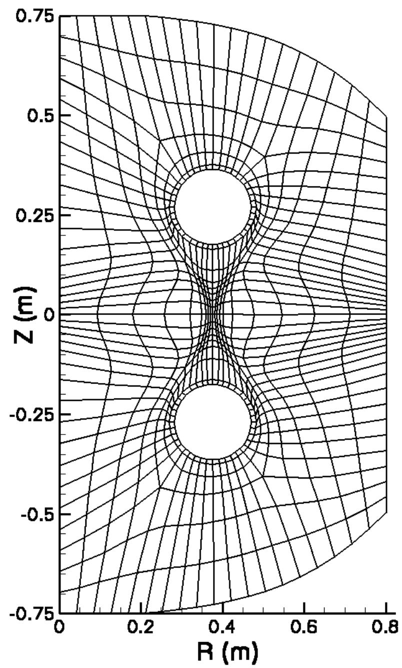

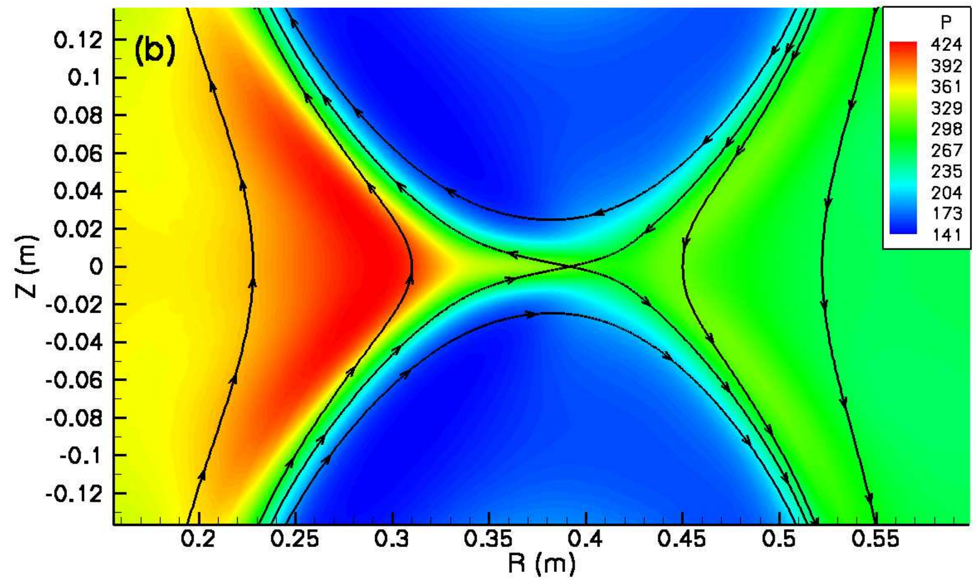

- Simulations of the Magnetic Reconnection Experiment (MRX) were performed in Murphy & Sovinec (2008)
- During the push mode of operation (similar to spheromak merging), a density buildup at low radii occurred because less volume was available on the inboard side of the current sheet than the outboard side, pushing the X-point towards higher radii and contributing to an asymmetric outflow pattern
- The position of the current sheet does not greatly vary because reconnection was driven through flux cores
- In linear geometry, the outer boundary is rectangular

Comparison of linear geometry MRX simulation to Eqs. 19–21

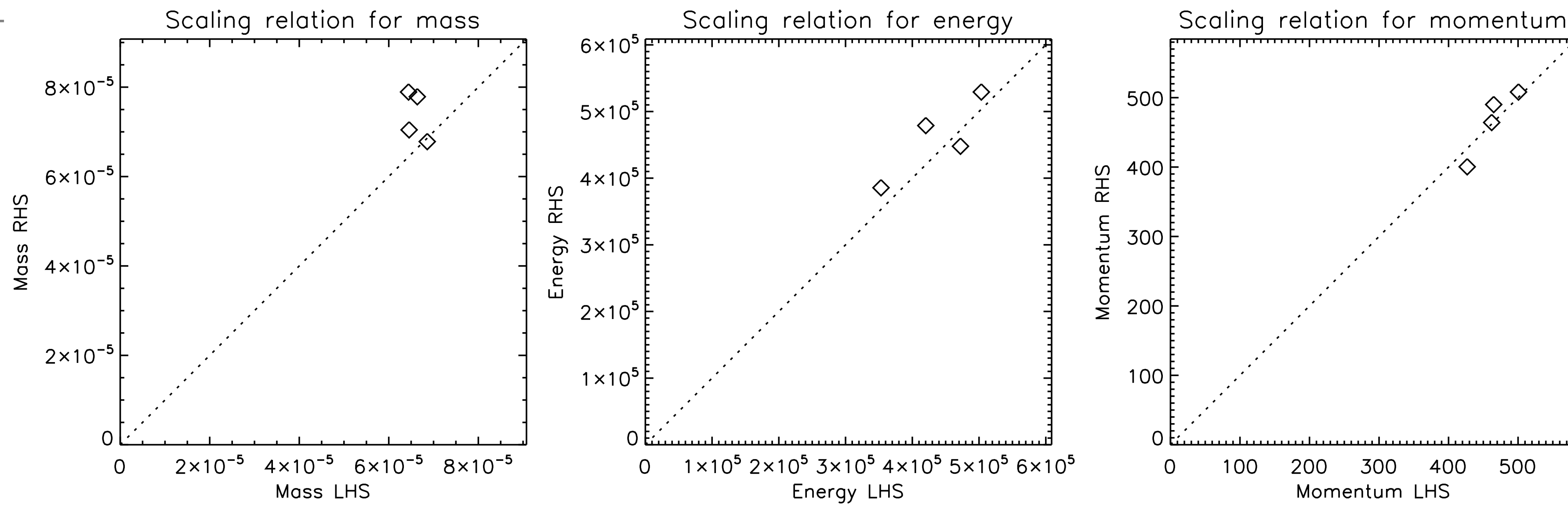

- We present comparisons of the conservation relations during a simulation of push reconnection in linear geometry using the setup of MRX where one wall is closer to the current sheet than the other wall
- Here and in the next slide, we calculate δ and $\mathcal{L}$ and choose values from when the current density falls by a factor of e from its peak value
- The data points represent different times during the same simulation
- Agreement with Eqs. 19–21 is good, especially considering the tension force in the downstream region is non-negligible

Comparison of toroidal geometry MRX simulation to Eqs. 40–42

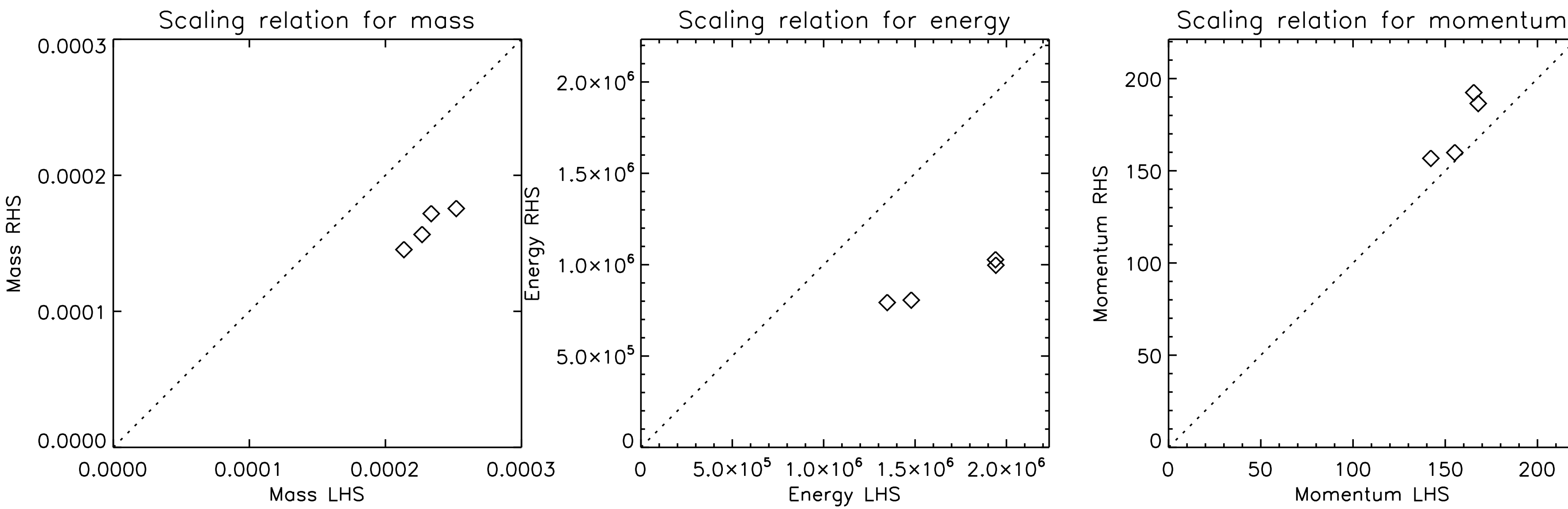

- We see fair agreement with conservation of mass and energy at different times during the push reconnection simulation reported in Murphy & Sovinec (2008)
- The discrepancy regarding conservation of mass is because the width of the current sheet increases further from the X-point
- The discrepancy regarding conservation of energy is because our assumed magnetic field profile overestimates the Poynting flux into the layer

Summary and Conclusions

- Magnetic reconnection with asymmetry in the outflow direction occurs in many situations in nature and the laboratory
- By using a surface integral approach, we derive scaling relationships that describe reconnection with asymmetric downstream pressure
- Reconnection is greatly slowed only when outflow from both sides of the current sheet is blocked because current sheet broadening reduces the bottleneck effect associated with conservation of mass
- A similar analysis is possible for toroidal geometry
  - In this case, it is possible to have quicker radially inward directed outflow than radially outward directed outflow even when the inboard pressure exceeds the outboard pressure
- NIMROD simulations show reasonably good agreement with our order of magnitude theory regarding conservation of mass, momentum, and energy
- Future work involves improving comparisons to simulation and investigating the current sheet interior